FSF 2019 – 3rd International Symposium on Fire Safety of Facades
Paris, France, September 26-27, 2019

NUMERICAL INVESTIGATION OF FIRE DEVELOPMENT IN A MEDIUM SCALE ISO9705 COMPARTMENT-FAÇADE CONFIGURATION

Antoine Afflard[1], El Mehdi Koutaiba[1], Eleni Asimakopoulou[2], Dionysios Kolaitis[3], Jianping Zhang[2], Paul Lardet[1]

[1] Universite Paris-Est, Centre Scientifique et Technique du Batiment (CSTB), France.
[2] FireSERT, School of Architecture and the Built Environment, Ulster University, UK.
[3] Laboratory of Heterogeneous Mixtures and Combustion Systems, School of Mechanical Engineering, National Technical University of Athens, Greece

ABSTRACT

This study aims to numerically investigate the fundamental physical phenomena governing fire development and transition to Externally Venting Flames (EVF) of liquid pool fires in compartment façade configurations. Experiments previously performed using a ¼ scale ISO9705 room with an extended façade is simulated using Fire Dynamics Simulator (FDS). The burning rate of the liquid n-hexane pool fire is modelled, and predictions of the compartment's interior thermal fields are compared with the experimental data showing good agreement in all considered test cases. A parametric study is also performed to examine the important physical parameters including the fire load and opening geometry, which govern the transition to EVF and their subsequent development in different phases. This work provides insights into best practice in numerical simulations that can be applied to model façade fires in the frame of performance-based design.

1 INTRODUCTION

Worldwide, development and implementation of performance-based codes are becoming a growing fire safety engineering trend. The utilization of performance-based codes requires the use of advanced fire simulation tools, such as zone or Computational Fluid Dynamics (CFD) models. These tools can provide a wealth of information regarding the detailed characteristics of the flow- and thermal-field developing at the interior and exterior of the fire compartment, characteristics of externally venting flames (EVF) and their thermal impact on the façade. Though numerous investigations have been conducted using CFD-based techniques to simulate fire development in compartment-façade configurations [1-4] there are scarce studies specifically focusing on the development and characterization of the resulting EVF in medium scale configurations and relevant façade fire safety issues [5-7]. Aiming at filling this gap, a numerical methodology has been developed to further investigate EVF development and its effect on the façade.
The effect of ventilation on the EVF development and the façade heat exposure has been assessed using numerical tools and the Eurocode methodology [8]. Both Forced and Natural Draught conditions have been investigated when studying the EVF characteristics in a corridor-compartment-façade configuration exposed to natural fire conditions, based on the large-scale experimental data provided by Klopovic and Turan [9]. Recently, a numerical study has been published [3] focusing on the appropriate use of fire barriers to prevent façade fires. Several different façade construction techniques have been studied with a special emphasis on the use of combustible insulation materials as part of the façade configuration. Numerical simulation results indicated that the use of combustible insulation materials significantly increased fire spreading. Aiming at filling this gap, a numerical methodology has been developed to assess the ability of currently available CFD tools to accurately describe fire development at the interior of an underventilated compartment and its effect on the characteristics of the EVF.

2 EXPERIMENTAL SETUP

2.1 Medium scale compartment-façade configuration

In that frame the Fire Dynamics Simulator (FDS) open source code (Version 6.5.3), has been used to simulate the turbulent, multi-component and reactive flow-field developing at the interior and exterior of a series of compartment-façade configurations. Numerical predictions are compared to the obtained experimental measurements from medium-scale fire tests as presented in detail previous research work of the authors [10]. The compartment was a ¼ scale model of an ISO 9705 compartment, *Fig. 1*. The internal compartment dimensions were 0.60 m x 0.90 m x 0.60 m; the external façade wall measured 0.658 m x 1.8 m. A double layer of 0.0125 m thick fireproof gypsum plasterboards was used as an internal and external lining material. A summary of the main operational parameters of the examined i.e. opening height (H), opening width (W), ventilation parameter ($AH^{1/2}$, with A being the area of the opening), ambient temperature (T_∞) and relative humidity (RH_∞), total fire duration (t_{dur}), fuel mass (m_f), total heat release (Q_{tot}), average heat release rate (HRR) at the interior of the fire compartment (Q_{ins}) and excess HRR (Q_{ex}) [10], for the examined test cases, is given in *Table 1*.

Table 1. Summary of main operational parameters for the examined test cases

	D-1.00L	D-2.35L	D-4.70L	W-2.35L	D-demo
H (m)	0.5	0.5	0.5	0.3	0.5
W (m)	0.2	0.2	0.2	0.2	0.2
$AH^{1/2}$ ($m^{5/2}$)	0.044721	0.044721	0.044721	0.026833	0.044721
T_∞ (°C)	25.8	26.7	26.5	26.4	20
RH_∞ (%)	42.0	42.0	47.0	36.0	40
t_{dur} (s)	372	525	595	659	120
m_f (kg)	0.655	1.539	6.078	1.539	-
Q_{tot} (kW)	79.0	132.0	233.0	105.0	200.0
Q_{ins} (kW)	-	106.5	106.5	49.35	62.3 for 15mm grid
Q_{ex} (kW)	-	25.5	126.5	55.65	137.7 for 15mm grid

2.2 Measurement equipment

The overall thermal behaviour of the compartment-façade configuration was investigated by measuring temperatures and heat fluxes at various locations. More specifically, 10 K-type 1.5 mm diameter thermocouples, located at the front (CF) and rear (CB) corner of the compartment and 4 thermocouples vertically distributed at the centerline of the opening were used to determine the thermal field developing at the interior of the compartment.

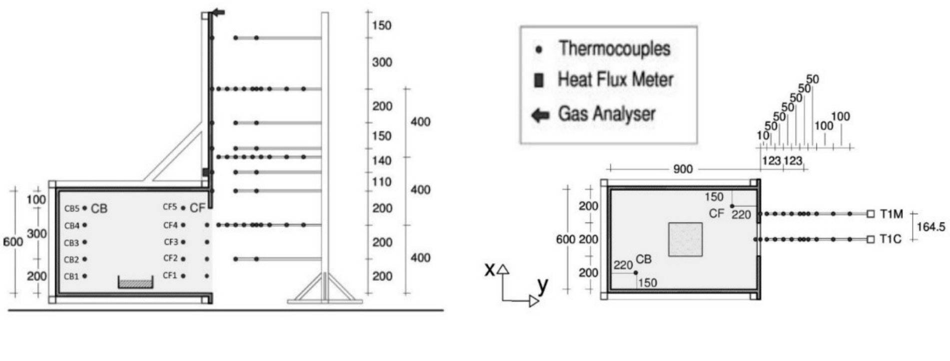

Fig. 1. Schematic drawing of the medium scale compartment façade ISO 9705 apparatus and sensor locations.

Emphasis was given to the characterization of the thermal environment adjacent to the façade wall along the height of the fire plume both in the centreline and off-axis positions 164.5 mm away from the centreline. Towards this end, 14 thermocouples were placed in various locations across the façade wall, whereas 27 additional thermocouples were distributed among two thermocouple trees as depicted in *Fig. 1*. All thermocouples measurements were recorded using a Universal Data Logging Interface designed in LabView software; the sampling frequency was 1 s [10]. The recorded thermocouple data, obtained at the interior of the compartment, were corrected for radiation using a "post-processing" methodology [10].

3 NUMERICAL SETUP

3.1 Simulation details: effect of grid size

A detailed review on grid resolution quality criteria enabled to perform a grid sensitivity study to compromise between model accuracy and computer capacity. Input data, assumed or based on experimental data, may introduce additional uncertainty into the model. Appropriate choice of the model geometry, resolution of the computational grid and boundary condition is essential and may define the analysis outcome. In order to treat these uncertainties, a grid sensitivity analysis was conducted for a demo case of the ¼ scale ISO 9705 geometry with a 0.2 m by 0.5 m opening with a prescribed constant HRR_{pre} of 200 kW. Eight different orthogonal meshes were used (7.5 mm, 10 mm, 15 mm, 20 mm, 25 mm, 30 mm, 35 mm and 40 mm cell sizes) and predictions of the temperature at positions CB and CF at the interior of the compartment are presented in *Fig. 2*. Predictions of the velocity profile in the opening are also presented.

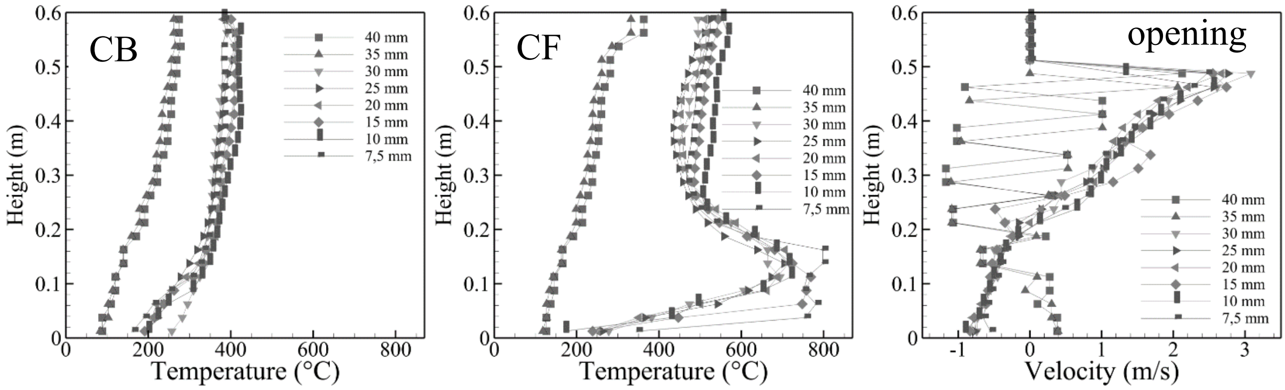

Fig. 2. Grid sensitivity results throughout comparison of gas temperature at the interior of the fire compartment at position CB (left), CF (middle) and velocity distribution at the opening (right) for test case D-demo.

The selected 15 mm cell size numerical grid is used in the control volume containing the fire room and the attached façade and the total number of computational cells is 388,800. In the general context of compartment fire simulations, the quality of the utilized grid resolution is commonly assessed using the non-dimensional $D^*/\delta x$ ratio, where D^* is a characteristic fire diameter and δx corresponds to the nominal size of the grid cell. The $D^*/\delta x$ ratio corresponds to the number of computational cells spanning D^* and is representative of the adequacy of the grid resolution. If the value of the $D^*/\delta x$ ratio is sufficiently large, the fire can be considered well resolved. Several studies have shown that values of 10 or more are required to adequately resolve most fires and obtain reliable flame temperatures [11]. The 15 mm cell size mess fulfils the $D^*/\delta x \geq 10$ criterion. At the beginning of the numerical simulation, the entire computational domain is assumed to be still (zero velocity), exhibiting a temperature of 20°C and the relative humidity is set at 40%. The "Very Large Eddy Simulation" mode of FDS has been used for the simulation cases. The time step is dynamically adjusted in order to satisfy the Courant-Friedrich-Levy (CFL) criterion [12]. The CFL condition asserts that the solution of the equations cannot be updated with a time step larger than that allowing a parcel of fluids to cross a grid cell according to *Eq. 1*. The exact CFL value needed to maintain stability depends on the order of the time integration scheme and the choice of the velocity norm [13].

The velocity norm value is set to unity, corresponding to the more restrictive L_1 norm for the velocity vector as depicted in *Eq. 2*, where δt is the time step and $\frac{\|\mathbf{u}\|}{\Delta}$ the velocity norm.

$$\mathrm{CFL} = \delta t \frac{\|\mathbf{u}\|}{\Delta} < 1 \tag{1}$$

$$\frac{\|\mathbf{u}\|}{\Delta} = \frac{|u|}{\delta x} + \frac{|v|}{\delta y} + \frac{|w|}{\delta z} + |\nabla \cdot \mathbf{u}| \tag{2}$$

The total simulation time is selected to be equal to the respective duration of each test case. Open boundaries are imposed at all boundaries external to the enclosure, with background species of ambient air and wall boundary conditions are used at walls, ceiling and floor. For the RTE, 104 control angles are used whereas time and angle increment are valued 3 and 5 respectively. Concerning the radiation solver for RADCAL calculations, it is assumed that the n-Heptane gas is used as surrogate to n-Hexane gas behaving as a grey medium with 0.125 m pathlength. In order to simulate the "realistic" fire condition of each test case, a variable mass loss rate according to available experimental data of fuel consumption rate has been used as the fire source by using mass-flux boundary condition. The soot yield, which represents the fraction of n-hexane fuel mass converted to smoke particulates, is set equal to 3.5% and the corresponding CO yield was set equal to 0.1 % [14]. Simulations are conducted using up to 500 CPU hours with a 3GHz processor.

3.2 Simulation details: effect of volume extension

The numerical grid extends to the outside of the enclosure, in order to effectively simulate air entrainment phenomena through the openings and burning outside the compartment. The size of the physical domain extending at the exterior of the fire compartment, is an important parameter that may influence the EVF development [15] and the temporal evolution at the interior of the compartment [16]. Six different cases have been investigated, by varying the external volume extension (ΔL); cases of ΔL values of 25 mm, 300 mm 500 mm and 700 mm are depicted in *Fig. 3* respectively.

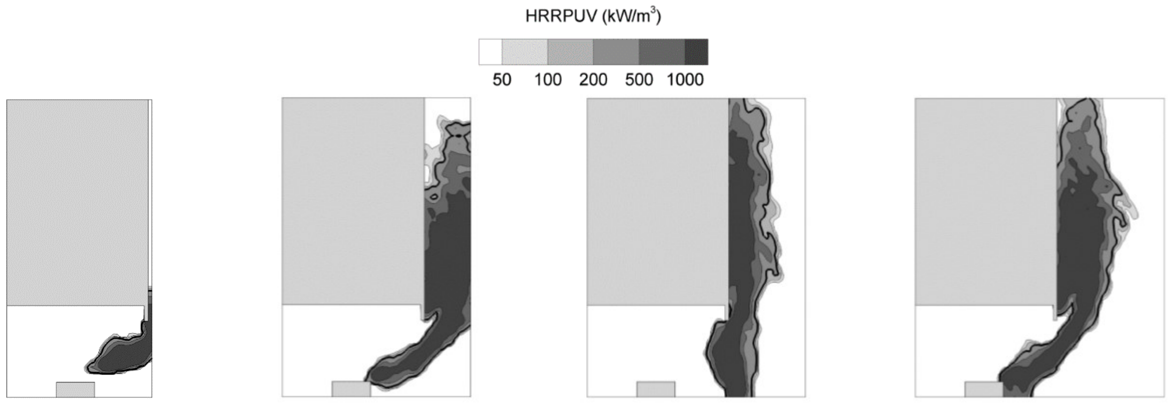

ΔL = 25 mm ΔL = 300 mm ΔL = 500 mm ΔL = 700 mm

Fig. 3. Predictions of the EVF envelope 94.8 s after fire initiation for test case D-demo with ΔL valued 25 mm, 300 mm, 500 mm and 700 mm.

The flames presence represented using the heat release rate per unit volume (HRRPUV) are displayed in Figure 3. A HRRPUV cutoff value of 200 kW/ m^3 (default value used by FDS to show flames) is also represented as a bold contour in the same figure. Relevant predictions of the gas temperature at different heights at the interior of the fire compartment in positions CB and CF are depicted in *Fig. 4*. Numerical results indicate that an external volume extension (ΔL) of 100 mm can be used to achieve "convergence". Based on those numerical results, a 100 mm grid extension has been applied in the x- and 30 mm in the z-direction respectively for test cases D-1.00L, D-2.35L, D-4.70L and W-2.35L respectively.

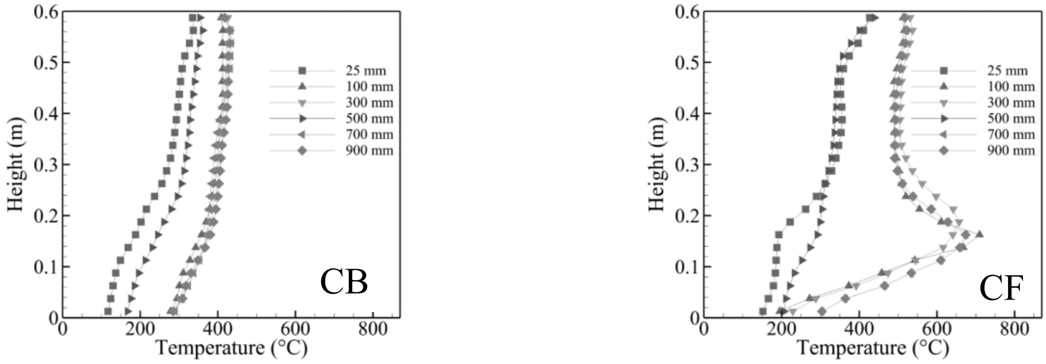

Fig. 4. Effect of the extension volume on the gas temperature at the interior of the fire compartment at position CB (left) and CF (right) for test case D-demo.

4 RESULTS AND DISCUSSION

4.1 Thermal field at the interior of the fire compartment

The temporal evolution of the gas temperatures at the interior of the compartment for every test case are presented in *Figs.* 5 and 6 respectively at heights from the ground: 0.1 m (CB1 and CF1), 0.3 m (CB3 and CF3) and 0.5 m (CB5 and CF5). Experimental measurements (Exp.) are compared to CFD predictions (FDS).

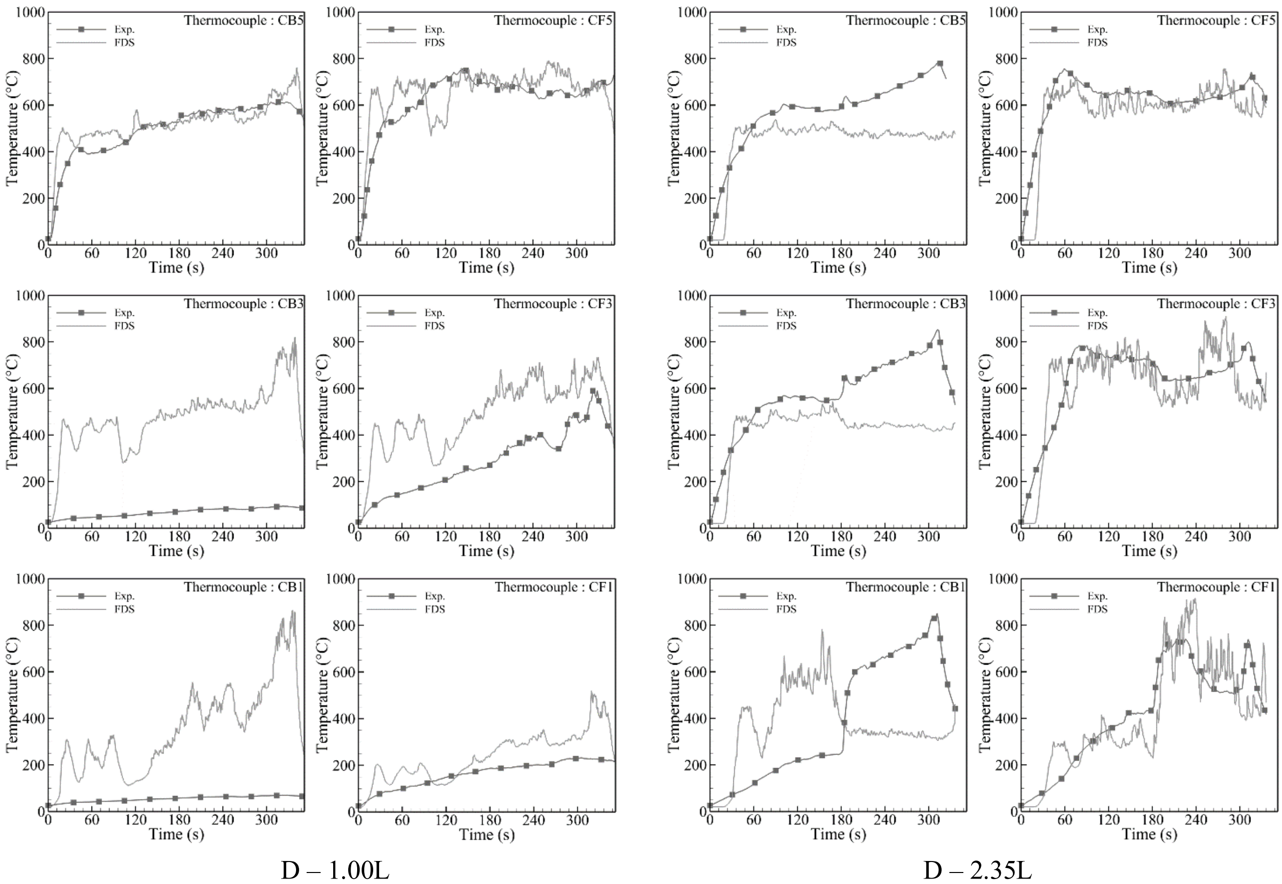

D – 1.00L D – 2.35L

Fig. 5. Temporal evolution of gas temperature at heights 0.1 m, 0.3 m and 0.5m from the ground for D-1.00L (left) and D-2.35L (right).

Generally, predictions of the gas temperature at the interior of the fire compartment show good levels of qualitative agreement with measured values. In test case D-1.00L, numerical results over-predict the gas temperature, particularly in the lower part and in the rear corner of the compartment. whereas in test cases D-2.35L, D-4.70L and W-2.35L, FDS tends to slightly under-predict the measured values. In *Fig. 6*, it can be seen for the case D – 4.70L that the two peaks observed experimentally at approximately 3 min and 8 min seems to be reproduced numerically with a time lag. This behaviour may be attributed to the difficulty of the FDS code to accurately predict the presence of combustion regions in the interior of the fire compartment in under-ventilated conditions [9] due to oxygen depletion, pertaining to the examined test cases. Combustion model in FDS assumes that fuel and oxygen burn instantaneously when mixed. This assumption may not be appropriate for incomplete combustion that commonly characterizes under-ventilated compartment fires.

4.2 EVF ejection and fire phases

As observed in all test cases, initially combustion is constrained in the interior of the fire compartment "internal flaming", IF phase, and in the vicinity of the fuel pan an advection stream is created. Gradually, the flame front moves away from the fuel pan, expanding radially and horizontally towards the opening. In that phase, external flame jets and quick flashes appear at the exterior of the fire compartment, signifying the beginning of the "intermittent flame ejection", IFE stage.

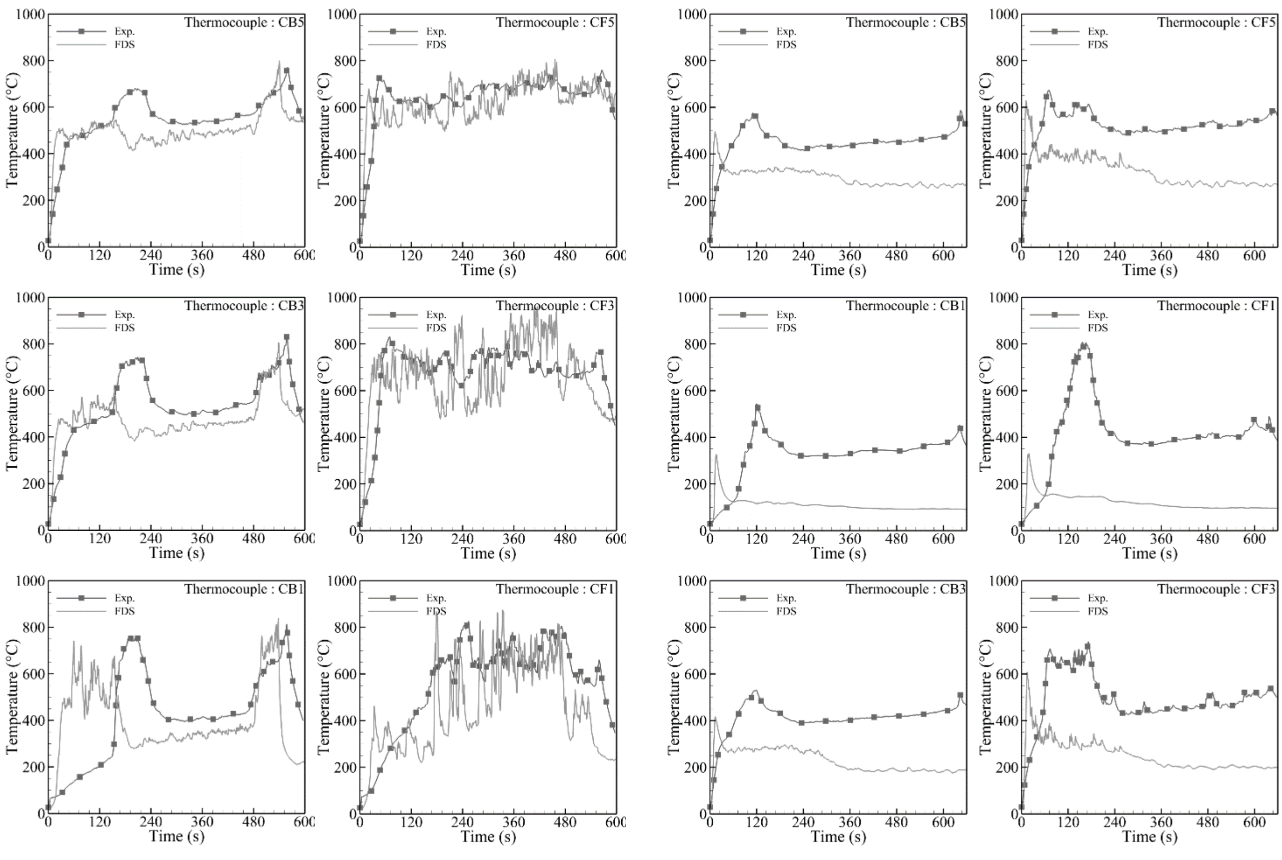

Fig. 6. Temporal evolution of gas temperature at heights 0.1 m, 0.3 m and 0.5m from the ground for D-4.70L (left) and

As time passes, "consistent external flaming", CEF phase, is observed due to the sustained external combustion of unburnt volatiles, during the quasi-steady phase of fully developed fire [9, 10]. Various parameters affect the development and duration of these phases in rectangular fire compartments, e.g. the effect of size of the opening [17] and the fuel type [18]. In order to further investigate the occurrence of each phase in relation to Q_{ins}, D-demo geometry has been used to simulate various test cases by applying a prescribed constant HRR_{pre} at the burner ranging from 30 kW to 330 kW. Relevant Q_{ins} values in relation to HRR_{pre} and the maximum HRR inside the enclosure according to Kawagoe correlation [17] is also plotted for comparison. IF phase is observed for up to 50kW, as Q_{ins} equals HRR_{pre}; an illustration is depicted in *Fig.* 8. From 60 kW to 140 kW a nearly constant value of Q_{ins} is observed and both IF and IFE phases are observed. During the IFE phase, between 170 and 190 kW, flames are located in the area between the burner and the opening. A new level of Q_{ins} is reached when HRR_{pre} values are greater than 200 kW and CEF phase is observed with oscillating EVF behaviour. When HRR_{pre} values are greater than 250 kW EVF behaviour is highly unpredictable and depends on numerical parameters. A correlation has been derived for Q_{ins} in relation to HRR_{pre} and ventilation parameter $AH^{1/2}$, as depicted in *Eq. 3*.

$$Q_{ins} = 925\,A\sqrt{H} \tag{3}$$

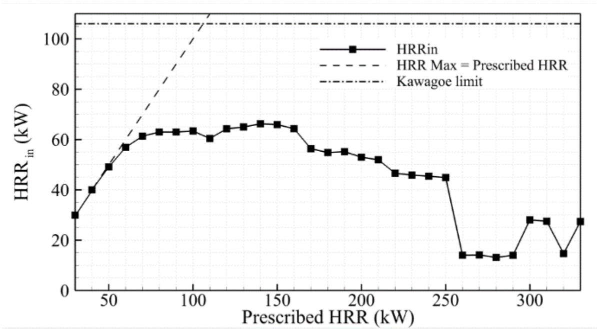

Fig. 7. Q_{ins} in relation to HRR_{pre}.

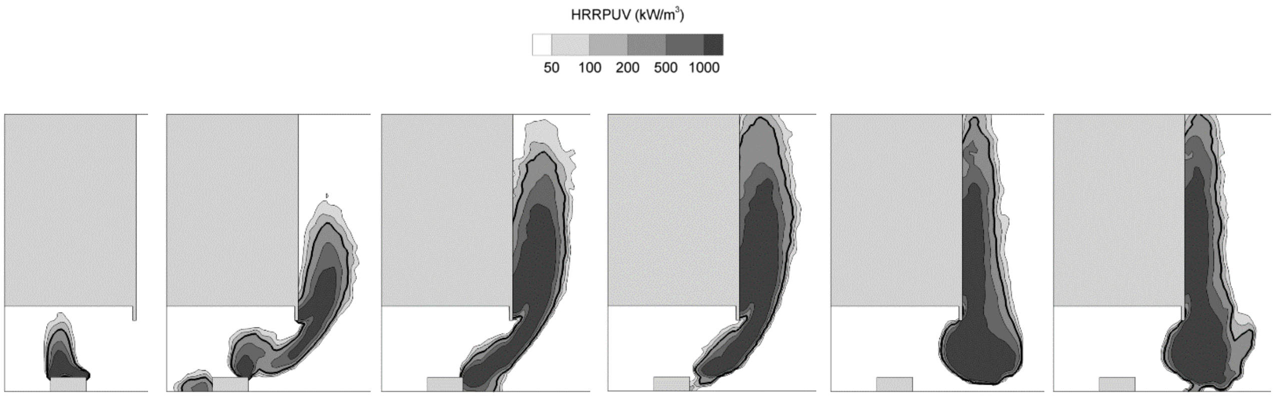

40 kW 110 kW 190 kW 220 kW 280 kW 290 kW

Fig. 8. Illustration of fire phases for different prescribed HRR_{pre}.

5 CONCLUSIONS

The dynamic nature of EVF requires the use of advanced modelling methodologies, capable of describing the relevant physical phenomena. The commonly used prescriptive methodologies are based on a phenomenological approach that exhibits certain limitations, especially when unusual structures are considered. CFD tools may provide significant assistance to the fire safety engineering analysis of EVF, by offering the opportunity to obtain an in-depth view of the spatial and temporal distribution of important physical parameters such as velocity, gas temperatures, wall temperatures, heat fluxes etc. In the current work, a series of medium scale compartment-façade fire tests were analysed numerically, aiming to investigate the effect of ventilation conditions in EVF development and fire phases. The obtained predictions are compared to available experimental data; good qualitative and, in certain cases, quantitative agreement is observed.

ACKNOWLEDGMENT

This study has been financially supported by the “Fire-Facts” project in the frame of the ARISTEIA action (operational program "Education and Lifelong Learning") that is co-financed by Greece and the E.U. and by the E.C. in the frame of two FP7 projects and "ELISSA: Energy Efficient Lightweight-Sustainable-Safe-Steel Construction" (EeB.NMP.2013-1, Grant No. 609086).

REFERENCES

[1] Nguyen Q.T., Tran P. Ngo T.D., Tran P.A., Mendis P., "Experimental and computational investigations on fire resistance of GFRP composite for building façade", Composites Part B: Engineering, 62, 218-229, 2014.
[2] Jahn W., Rein G., Torero J. L., "The effect of model parameters on the simulation of fire dynamics", Fire Safety Science, 9, 1341-1352, 2008.
[3] Giraldo P.M., Lacasta A., Avellaneda J., Burgos C., "Computer simulation on fire behaviour in the ventilated cavity of ventilated façade systems", MATEC Web of Conferences 9, 03002, 2013.
[4] Martinez B.R., "Contribution to the study by numerical simulation of a fire plume coming out through a window on façade: Application to the comprehension of the wind influence on an eventually stack effect", MATEC Web of Conferences, Volume 9, Article 03004, found in Proceedings of the 1st International Seminar for Fire Safety of Facades, Paris, France, 14-15 November 2013.
[5] Wang H.Y., "Numerical study of under-ventilated fire in medium-scale enclosure", Building and Environment, 44, 1215-1227, 2009.
[6] Mammoser J.H., Battaglia F., "A computational study on the use of balconies to reduce flame spread in high-rise apartment fire", Fire Safety Journal, 39, 277-296, 2004.
[7] Meunders A., Trettin C., Wittbecker F., "The capability of FDS to model flames and plumes emerging from compartment openings", Proceedings of the International Congress of Fire Computer Modelling, 457-470, Santander, Spain, 18-19 October, 2012.
[8] Asimakopoulou E.K., Kolaitis D.I., Founti M.A., "Assessment of fire engineering design correlations used to describe the geometry and thermal characteristics of Externally Venting Flames", Fire Technology, 2016.
[9] Klopovic S., Turan O.F., "A comprehensive study of externally venting flames, Part I: Experimental plume characteristics for through-draft and no through-draft ventilation conditions and repeatability", Fire Safety Journal, 36, 99-133, 2001.
[10] Asimakopoulou E.K., Chotzoglou K., Kolaitis D.I., Founti M.A., "Characteristics of Externally Venting Flames and their effect on the façade: a detailed experimental study", Fire Technology, 2016.
[11] Lin C.H., Ferng Y.M., Hsu W.S., "Investigating the effect of computational grid sizes on the predicted characteristics of thermal radiation for a fire", Applied Thermal Engineering 29, 2243-2250, 2009.
[12] McGrattan K., Hostikka S., McDermott R., Floyd J., Vanella M., "Fire Dynamics Simulator User’s Guide", NIST Special Publication 1019, 6th Edition, 2019.
[13] McGrattan K., Hostikka S., McDermott R., Floyd J., Vanella M., "Fire Dynamics Simulator Technical Reference Guide Volume 1: Mathematical Model", NIST Special Publication 1018-1, 6th Edition, 2019.
[14] Tang F., Hu L., Wang Q., Lu K.H., Yang L.Z., "An experimental investigation on temperature profile of buoyant spill plume from under-ventilated compartment fires in a reduced pressure atmosphere at high altitude", Intenrational Journal of Heat and Mass Transport 55, 5642-5649, 2012.
[15] Zhang, X., Yang, M., Wang, J., He, Y., "Effects of computational domain on numerical simulation of building fires", Journal of Fire Protection Engineering, 20, 225-250, 2010.
[16] He Y., Jamieson C., Jeary A., Wang J., "Effect of computational domain on simulation of small compartment fires", Fire Safety Science Proceedings of 9th International Symposium, 1365-1376, 2008.
[17] Kawagoe K., Fire Behaviour in Rooms, Report No 27, Building Research Institute, Tokyo, Japan, 1958.
[18] Delichatsios M.A., Silcock, G.W.H., "Fully involved enclosure fires: effects of fuel type, fuel area and geometry", Proceedings of 7th International Symposium of Fire Safety Science, 59-73, 2002.